ChemComm

COMMUNICATION

View Article Online
View Journal | View Issue

Cite this: *Chem. Commun.*, 2021, 57, 733

Received 12th November 2020,
Accepted 11th December 2020

DOI: 10.1039/d0cc07446b

rsc.li/chemcomm

Insights into D_{4h}@metal-symmetry single-molecule magnetism: the case of a dysprosium-bis(boryloxide) complex†

Lewis R. Thomas-Hargreaves, [a] David Hunger,[b] Michal Kern,[b] Ashley J. Wooles,[a] Joris van Slageren, [b] Nicholas F. Chilton *[a] and Stephen T. Liddle *[a]

We report the synthesis of the lanthanide-(bis)boryloxide complex [Dy{OB(NArCH)$_2$}$_2$(THF)$_4$][BPh$_4$] (2Dy, Ar = 2,6-Pr$^i_2$C$_6$H$_3$), with idealised D_{4h}@Dy(III) point-group symmetry. Complex 2Dy exhibits single-molecule magnetism (SMM), with one of the highest energy barriers (U_{eff} = 1565(298) K) of any six-coordinate lanthanide-SMM. Complex 2Dy validates electrostatic model predictions, informing the future design of lanthanide-SMMs.

With potential applications in quantum technologies and high-density data storage, the field of lanthanide (Ln) single-molecule magnetism (SMM) has expanded rapidly in recent years due to large energy barriers to reversal of magnetisation (U_{eff}) and blocking temperatures (T_B).[1] The principal factor controlling the performance of Ln-SMM is the crystal field (CF), and, following intuitive electrostatic principles, strong uniaxial CFs for Dy(III) stabilise the largest projections of the total angular momentum, $m_J = \pm 15/2$, which has an oblate spheroidal electron density distribution.[2] Thus, there has been great interest in controlling the symmetry of the coordination sphere of Dy(III) complexes to engineer improved SMM performance.[3] However, Ln-SMM is often subject to zero-field quantum tunnelling of the magnetization (QTM) that can bypass the anisotropy barrier, which is known to relate to hyperfine coupling and dipolar fields, but may also relate to spin-phonon coupling.[4]

As a result of the development of the electrostatic model,[5] developing different geometries and thus metal point group symmetries has become a burgeoning area of investigation because some point groups prevent transverse CF terms by symmetry,[6] meaning that the prevalence of QTM processes should be greatly diminished. Complexes with S_8/D_{4d},[7] C_{5h}/D_{5h},[3d,8] S_{12}/D_{6d}, D_{6h},[9] and C_n (where $n \geq 7$)[10] have been found to be particularly effective. However, Ln-SMM complexes with D_{4h}@Dy(III) symmetry at the metal remain rare,[11] a vexatious situation considering the dominance of O_h and D_{4h} complexes in coordination chemistry in general.

Around twenty (pseudo) O_h and D_{4h}@Dy-SMM complexes are known, but few exhibit U_{eff} values >700 K: notable examples include [Dy(BIPM)$_2$]$^-$ (721/813 K),[12] [Dy{NC(NArCH)$_2$}(Cl)$_2$(THF)$_3$] (803 K, Ar = 2,6-Pr$^i_2$C$_6$H$_3$),[13] [Dy(Cy$_3$PO)$_2$(I)$_3$(CH$_3$CN)] (1062 K),[14] [Dy(DiMeQ)$_2$(Cl)$_3$(H$_2$O)] (1100 K),[15] and recently [Dy(OBu^t)$_2$(Py-4-R)$_4$]$^+$ (1810–2075 K, R = Ph, N(CH$_2$CH$_2$)$_2$CH$_2$, N(CH$_2$CH$_2$)$_2$).[16] For D_{4h}@Dy(III) SMMs, the latter three bis(alkoxide) complexes exhibit remarkable U_{eff} values, yet conversely D_{4h}@Dy(III) [Dy(carbazolyl)$_2$(L)$_4$]$^+$ (L = py, THF) exhibit U_{eff} barriers of 57–72 K.[17] This is surprising because electrostatic models predict that [Dy(X)$_2$(THF)$_4$]$^+$ (X = monoanionic ligand) species should exhibit U_{eff} values of ~860–1500 K.[5] The experimental D_{4h}@Dy(III) U_{eff} variance of ~2000 K suggests that much remains to be understood in electrostatic models, and so further data are required to validate or modify electrostatic potential theory.

Monoanionic O-donor ligands have proven particularly effective in Dy-SMM complexes. Our attention was drawn to the boryloxide ligand $^-$OB(NArCH)$_2$, which is isoelectronic to the imine $^-$NC(NArCH)$_2$ ligand used in [Dy{NC(NArCH)$_2$}(Cl)$_2$(THF)$_3$].[13] Though boryloxide ligands are poorer donors compared to the NH-imine, we surmised that a Dy-bis(boryloxide) complex could provide a high performance D_{4h}@Dy(III) SMM complex to compare to electrostatic model predictions. Further motivation stemmed from the fact that *N*-substituted Ln–boryloxide complexes are rare, and have resulted from tris(pyrazoyl)borate decomposition rather than from targeted syntheses.[18] Here, we present the realisation of our goal, which has resulted in a D_{4h}@Dy(III) complex with one of the largest U_{eff} values to date. These results inform the electrostatic model and thus could assist the targeted design of improved lanthanide SMM.

[a] *Department of Chemistry, The University of Manchester, Oxford Road, Manchester, M13 9PL, UK. E-mail: steve.liddle@manchester.ac.uk, nicholas.chilton@manchester.ac.uk*

[b] *Institute of Physical Chemistry, University of Stuttgart, Pfaffenwaldring 55, Stuttgart, D-70569, Germany*

† Electronic supplementary information (ESI) available: Experimental and computational details. CCDC 2043760–2043763. For ESI and crystallographic data in CIF or other electronic format see DOI: 10.1039/d0cc07446b

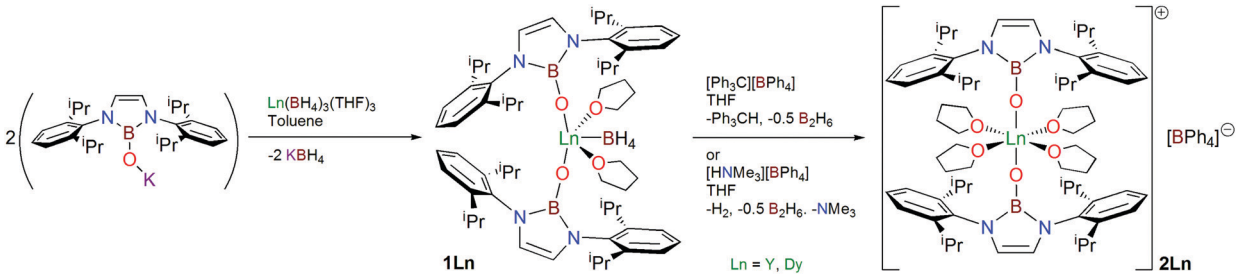

Scheme 1 Synthesis of **1Ln** and **2Ln** (Ln = Dy, Y).

Treatment of $[Dy(BH_4)_3(THF)_3]$[19] with two equivalents of $[KOB(NArCH)_2]$[20] in toluene proceeds with elimination of KBH_4 to give, after work-up, the dysprosium bis(boryloxide) complex $[Dy\{OB(NArCH)_2\}_2(BH_4)(THF)_2]$ (**1Dy**), isolated as colourless crystals in 86% yield, Scheme 1.[21] Following isolation, the coordinated BH_4^- group can be replaced with the non-coordinating BPh_4^- anion, using $[Ph_3C][BPh_4]$ or $[HNMe_3][BPh_4]$, in THF, to produce $[Dy\{OB(NArCH)_2\}_2(THF)_4][BPh_4]$ (**2Dy**), Scheme 1. Both routes are synthetically effective, with isolated crystalline yields of **2Dy** of 77 and 94%, respectively, though the latter route is more practicable not only for increased yield compared to the former but because gaseous by-products are formed, simplifying work-up. To give confidence in the formulations of **1Dy** and **2Dy** we also prepared the yttrium analogues **1Y** and **2Y**. Attempts to abstract the BH_4^- group from **1Ln** in non-polar solvents did not give crystalline material, but subsequent addition of THF and recrystallisation gave **2Ln**.

The ^{1}H, ^{11}B, and ^{13}C NMR spectra of **1Y** and **2Y** are consistent with their structures, with the BH_4^- ligand in **1Y** (^{11}B δ −28.4 ppm) clearly being replaced by the BPh_4^- anion in **2Y** (^{11}B δ −6.5 ppm), though the characteristic boryl resonance is virtually unshifted from **1Y** to **2Y** (^{11}B δ 21.5, 21.6 ppm, respectively).[21] The IR spectra of **1Y** and **1Dy** exhibit absorptions that are characteristic of an ionic coordination mode of BH_4^-, and their absence in the corresponding spectra of **2Y** and **2Dy** is consistent with the exchange of BPh_4^- for BH_4^-.

The solid-state structure of **2Dy** was determined by single crystal X-ray diffraction and is shown in Fig. 1. The compound crystallises as a separated ion pair where the cation features a pseudo-octahedral Dy ion[22] with two axial *trans* boryloxide and four equatorial THF ligands. In the crystal examined, the shortest Dy···Dy interaction is 13.9151(6) Å. There is formally a C_2 rotation axis passing through O2–Dy–O4 and a vertical mirror plane passing through the O2–O1–O4–O1A plane (hence there is disorder in the structure), but the complex is very close to D_{4h} point symmetry at the metal: the O1–Dy–O1A angle is 175.9(3)° and the O1–Dy–O2/3/4 angles range from 86.2(7) to 94.5(7)°. The unique **2Dy** Dy–O1 bond length is 2.136(5) Å, which is slightly longer than the Dy–O_B distances of 2.089(10)/2.113(11) Å in **1Dy**, which likely reflects the absence of a fourth equatorial donor in **1Dy** compared to **2Dy**. Unsurprisingly, in **2Dy** the Dy–O2/3/4 bond lengths are considerably longer, ranging from 2.346(9) to 2.365(8) Å. Interestingly, the two boryloxide ligands tilt towards each other on one side of the complex

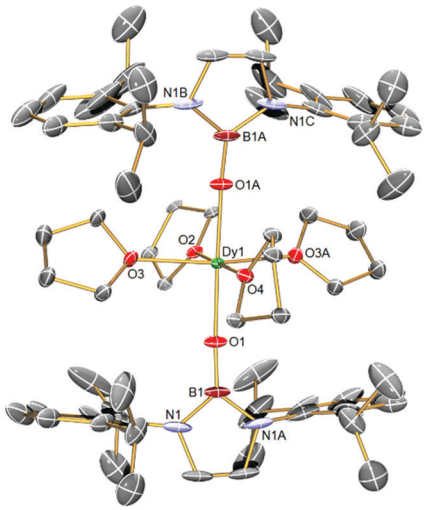

Fig. 1 Solid state structure of the cation component of **2Dy** at 150 K and displacement ellipsoids set to 40%. The BPh_4^- anion, hydrogen atoms, and THF disorder components are omitted for clarity.

(removing the putative C_4 rotation axis), with B–O–Dy angles of 169.7(5)°, but despite the tilting the B–O distance of 1.367(10) Å is statistically indistinguishable to other complexes. Although in many regards the structures of **2Dy** and **2Y** are very similar, we note a key difference, which is in **2Dy** the two boryloxide ligands adopt an eclipsed arrangement, whereas in **2Y** they are arranged orthogonally and so **2Dy** and **2Y** are not isostructural with one another, which prevents meaningful magnetic doping dilution experiments in this case.

The $\chi_M T$ value of 14.71 cm^3 mol^{-1} K for **2Dy** at 298 K is indicative of a single Dy(III) ion (expected 14.2 cm^3 mol^{-1} K) (Fig. S13, ESI†). This decreases only moderately until below 20 K where it falls precipitously to *ca.* 6 cm^3 mol^{-1} K at 1.8 K. In zero direct current field, alternating current susceptibility data for **2Dy** reveal peaks in the out-of-phase component up to 86 K (Fig. S15–S18, ESI†). Fitting these data to a generalised Debye model using the CC-FIT2 code[23] gives relaxation rates and distribution parameters which we convert to estimated standard deviations (esds);[24] note there is a high-frequency relaxation process that appears just above the frequency window of our instrument below 16 K, and so we fit the data using a two-process model but disregard the data for the poorly-defined fast-process. Fitting the temperature dependence of the magnetic

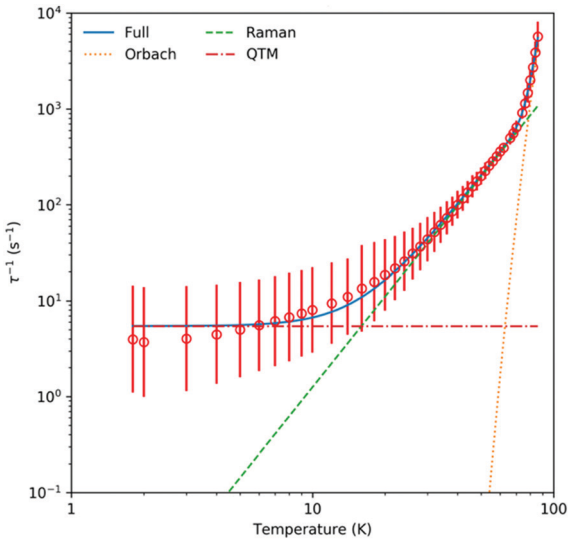

Fig. 2 Temperature dependence of magnetic relaxation rates for **2Dy** measured with alternating current susceptometry with zero direct current field.

relaxation rates with the expression $\tau^{-1} = \tau_0^{-1}\exp[-U_{eff}/kT] + CT^n + \tau_{QTM}^{-1}$ gives U_{eff} = 1565(298) K, $\tau_0 = 10^{-11.6(1.6)}$ s, $C = 10^{-3.05(0.45)}$ s^{-1} K^{-n}, n = 3.14(0.25), $\tau_{QTM} = 10^{-0.74(0.16)}$ s, Fig. 2. This indicates a very large Orbach relaxation barrier, surpassed only by a handful of compounds[3a–f] and one D_{4h} SMM (within esds);[16] here the large uncertainty in the U_{eff} barrier is due to the limited temperature range over which the exponential relaxation process is observed coupled with the esds from the generalised Debye model. Magnetic hysteresis experiments performed from 1.8 to 15 K with a sweep-rate of ~20 Oe s^{-1} reveal butterfly curves up to around 7 K, Fig. 3, however these are all closed at zero field, indicating efficient quantum tunnelling of the magnetisation.

Complete active space self-consistent field spin–orbit (CASSCF-SO) calculations using the crystallographic coordinates of the cation in **2Dy** show, Fig. 4, that the ground Kramers doublet is 97% $m_J = \pm 15/2$ with effective g-values $g_x = g_y = 0$, g_z = 19.86 (Table S2, ESI†). The first excited state at 763 K, whilst a mixture of

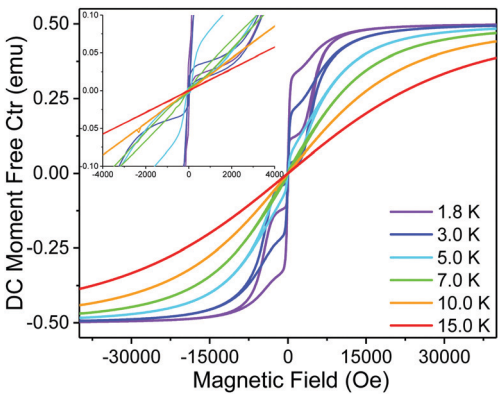

Fig. 3 Magnetic hysteresis measurements performed **2Dy** with a sweep rate of ~20 Oe s^{-1}. Inset shows a zoom around 0 field to show closing of hysteresis loops.

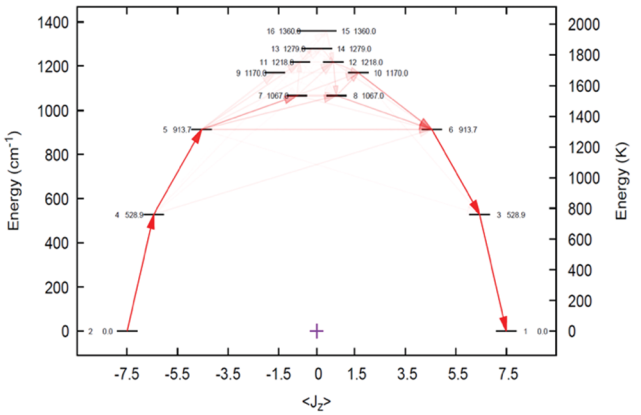

Fig. 4 CASSCF-SO CF splitting of the cation in **2Dy**. Arrows are likely Orbach transitions (av. Cartesian magnetic dipole operators); propensity is proportional to opacity.

70% $m_J = \pm 13/2$ and 28% $m_J = \mp 13/2$, retains very small transverse g-values (g_x = 0.05, g_y = 0.06, g_z = 16.83), and the second excited state at 1309 K is dominated by 87% $m_J = \pm 11/2$, but here the transverse g-values grow (g_x = 0.63, g_y = 1.08, g_z = 13.15); however, both first and second excited states share a common main magnetic axis with that of the ground state, deviating by 2.3° and 7.7°, respectively. However, the third excited state at 1536 K is very mixed (28% $m_J = \pm 1/2$, 26% $m_J = \mp 1/2$, 18% $m_J = \pm 9/2$, 11% $m_J = \mp 9/2$), has very large transverse g-values (g_x = 3.53, g_y = 6.79, g_z = 11.18), and its main magnetic axis is roughly orthogonal to that of the ground state (84.1° deviation). Thus, *ab initio* calculations predict relaxation *via* the Orbach process to occur through the third excited state, which is in excellent agreement with the experimental U_{eff}.

The U_{eff} and electronic structure of **2Dy** can be compared to the theoretical models of $[Dy(R)_2(THF)_4]^+$ (R = $N(SiH_3)_2$, $CH(SiH_3)_2$, $C(SiH_3)_3$), which were computed in a study examining the effects of linearity on U_{eff} and the effects of coordinated solvent and complex geometry.[5b] Pseudo-D_{4h} symmetry was predicted to have a U_{eff} barrier of ~1000 K for R = $(H_3Si)_2N^-$ and $(H_3Si)_2(H)C^-$, and 1600 K when R = $(H_3Si)_3C^-$. Considering the approximations made, these predictions are rather accurate.

Relaxation of the magnetisation occurs *via* the third excited state for **2Dy** as well as the $[Dy(OBu^t)_2(Py\text{-}4\text{-}R)_4]^+$ series, but the latter can have larger U_{eff} values; it is clear that shorter axial Dy–O distances (~2.066(8)–2.122(5) Å) linearly expand the energy range of the excited m_J state manifold,[16] but equatorial ligand coordination is still important. So, we compared the computed charges for the $[Dy(OBu^t)_2(Py\text{-}4\text{-}R)_4]^+$ series and **2Dy**; we find that the Dy, O, and N calculated LoProp charges for the former are 2.47 to 2.50, −1.09 to −1.12, and −0.39 to −0.40, and for **2Dy** the Dy, O_{Boryl}, and O_{THF} LoProp charges are 2.57, −1.02, and −0.56, respectively. These data suggest that the Dy atom in **2Dy** is more positively charged as a result of less charge donation from the ligands overall, but the boryloxide ligands are weaker donors than the alkoxides and the THF ligands are stronger donors than the pyridine ligands resulting in a weaker axial and greater equatorial ligand field for **2Dy** compared to the $[Dy(OBu^t)_2(Py\text{-}4\text{-}R)_4]^+$ series, which is in-line with the

observed U_{eff} data. Thus, whilst bond distances are a useful gross guide to likely magnetic performance, the potential donor strength of individual ligands is also a key factor within a range of effectiveness bracketed by the gross Dy–ligand distances.

To conclude, we have reported the synthesis of rare examples of Ln–boryloxide complexes utilising a borohydride elimination methodology. Complex **2Dy** is a D_{4h}@Dy(III) SMM with a large U_{eff} barrier likely surpassed by only one other D_{4h}@Dy(III) SMM. These results validate the electrostatic model, but also clarify an appreciation that charges and thus donor strength of ligands is an important criterion for SMM performance within the framework of Dy–ligand distances.

We thank the EPSRC (EP/P002560/1, EP/P001386/1, EP/M0270 15/1), ERC (CoG612724, StG851504), Royal Society (University Research Fellowship to NFC), German DFG (SL104/10-1), and The Universities of Manchester and Stuttgart for support.

Conflicts of interest

There are no conflicts to declare.

Notes and references

1 (*a*) Z. Zhu, M. Guo, X.-L. Li and J. Tang, *Coord. Chem. Rev.*, 2019, **378**, 350; (*b*) K. L. M. Harriman, D. Errulat and M. Murugesu, *Trends Chem.*, 2019, **1**, 425; (*c*) A. K. Bar, P. Kalita, M. K. Singh, G. Rajaraman and V. Chandrasekhar, *Coord. Chem. Rev.*, 2018, **367**, 163; (*d*) M. Feng and M.-L. Tong, *Chem. – Eur. J.*, 2018, **24**, 7574; (*e*) S. G. McAdams, A.-M. Ariciu, A. K. Kostopoulos, J. P. S. Walsh and F. Tuna, *Coord. Chem. Rev.*, 2017, **346**, 216; (*f*) S. T. Liddle and J. van Slageren, *Chem. Soc. Rev.*, 2015, **44**, 6655.

2 J. Sievers, *Z. Phys. B: Condens. Matter*, 1982, **45**, 289.

3 (*a*) Y.-S. Ding, T. Han, Y.-Q. Zhai, D. Reta, N. F. Chilton, R. E. P. Winpenny and Y.-Z. Zheng, *Chem. – Eur. J.*, 2020, **26**, 5893; (*b*) Z. Zhu and J. Tang, *Top. Organomet. Chem.*, 2019, **64**, 191; (*c*) K. R. McClain, C. A. Gould, K. Chakarawet, S. J. Teat, T. J. Groshens, J. R. Long and B. G. Harvey, *Chem. Sci.*, 2018, **9**, 8492; (*d*) F.-S. Guo, B. M. Day, Y.-C. Chen, M.-L. Tong, A. Mansikkamäki and R. A. Layfield, *Science*, 2018, **362**, 1400; (*e*) C. A. P. Goodwin, F. Ortu, D. Reta, N. F. Chilton and D. P. Mills, *Nature*, 2017, **548**, 439; (*f*) Y.-S. Ding, N. F. Chilton, R. E. P. Winpenny and Y.-Z. Zheng, *Angew. Chem., Int. Ed.*, 2016, **55**, 16071; (*g*) *Lanthanide Single Molecule Magnets*, ed. J. Tang and P. Zhang, Springer-Verlag, Berlin, Heidelberg, 2015; (*h*) N. F. Chilton, D. Collison, E. J. L. McInnes, R. E. P. Winpenny and A. Soncini, *Nat. Commun.*, 2013, **4**, 2551J; (*i*) D. Rinehart and J. R. Long, *Chem. Sci.*, 2011, **2**, 2078.

4 (*a*) K. Irländer and J. Schnack, *Phys. Rev. B*, 2020, **102**, 054407; (*b*) F. Ortu, D. Reta, Y.-S. Ding, C. A. P. Goodwin, M. P. Gregson, E. J. L. McInnes, R. E. P. Winpenny, Y.-Z. Zheng, S. T. Liddle, D. P. Mills and N. F. Chilton, *Dalton Trans.*, 2019, **48**, 8541; (*c*) E. Moreno-Pineda, G. Taran, W. Wernsdorfer and M. Ruben, *Chem. Sci.*, 2019, **10**, 5138; (*d*) Y.-S. Ding, K.-X. Yu, D. Reta, F. Ortu, R. E. P. Winpenny, Y.-Z. Zheng and N. F. Chilton, *Nat. Commun.*, 2018, **9**, 3134; (*e*) Y.-C. Chen, J.-L. Liu, W. Wernsdorfer, D. Liu, L. F. Chibotaru, X.-M. Chen and M.-L. Tong, *Angew. Chem., Int. Ed.*, 2017, **56**, 4996; (*f*) F. Pointillart, K. Bernot, S. Golhen, B. Le Guennic, T. Guizouarn, L. Ouahab and O. Cador, *Angew. Chem., Int. Ed.*, 2015, **54**, 1504; (*g*) N. Ishikawa, M. Sugita and W. Wernsdorfer, *J. Am. Chem. Soc.*, 2005, **127**, 3650.

5 (*a*) L. Ungur and L. F. Chibotaru, *Inorg. Chem.*, 2016, **55**, 10043; (*b*) N. F. Chilton, *Inorg. Chem.*, 2015, **54**, 2097; (*c*) M. A. Aldamen, J. M. Clemente-Juan, E. Coronado, C. Marti-Gastaldo and A. Gaita-AriÇo, *J. Am. Chem. Soc.*, 2008, **130**, 8874; (*d*) N. F. Chilton, D. Collison, E. J. L. McInnes, R. E. P. Winpenny and A. Soncini, *Nat. Commun.*, 2013, **4**, 2551; (*e*) Y. Bi, Y.-N. Guo, L. Zhao, Y. Guo, S.-Y. Lin, S.-D. Jiang, J. Tang, B.-W. Wang and S. Gao, *Chem. – Eur. J.*, 2011, **17**, 12476–12481; (*f*) S. D. Jiang, B. W. Wang, H. L. Sun, Z. M. Wang and S. Gao, *J. Am. Chem. Soc.*, 2011, **133**, 4730.

6 (*a*) J.-L. Liu, Y.-C. Chen and M.-L. Tong, *Chem. Sci.*, 2018, **47**, 2431; (*b*) L. Sorace, C. Benelli and D. Gatteschi,, *Chem. Soc. Rev.*, 2011, **40**, 3092; (*c*) C. Görller-Walrand and K. Binnemans, in *Handbook on the Physics and Chemistry of Rare Earths*, Elsevier, 1996, vol. 23.

7 Recent S_8/D_{4d} examples: (*a*) K. Katoh, S. Yamashita, N. Yasuda, Y. Kitagawa, B. K. Breedlove, Y. Nakazawa and M. Yamashita, *Angew. Chem., Int. Ed.*, 2018, **57**, 9262; (*b*) J. Wu, J. Jung, P. Zhang, H. Zhang, J. Tang and B. L. Guennic, *Chem. Sci.*, 2016, **7**, 3632.

8 Recent C_{5h}/D_{5h} examples: (*a*) A. B. Canaj, M. K. Singh, C. Wilson, G. Rajaraman and M. Murrie, *Chem. Commun.*, 2018, **54**, 8273; (*b*) Y.-C. Chen, J.-L. Liu, Y. Lan, Z.-Q. Zhong, A. Mansikkamaki, L. Ungur, Q.-W. Li, J.-H. Jia, L. F. Chibotaru, J.-B. Han, W. Wernsdorfer, X.-M. Chen and M.-L. Tong, *Chem. – Eur. J.*, 2017, **23**, 5708; (*c*) Y.-C. Chen, J.-L. Liu, L. Ungur, J. Liu, Q.-W. Li, L.-F. Wang, Z.-P. Ni, L. F. Chibotaru, X.-M. Chen and M.-L. Tong, *J. Am. Chem. Soc.*, 2016, **138**, 2829.

9 Recent D_{6h} examples: (*a*) J. Li, S. Gomez-Coca, B. S. Dolinar, L. Yang, F. Yu, M. Kong, Y.-Q. Zhang, Y. Song and K. R. Dunbar, *Inorg. Chem.*, 2019, **58**, 2610; (*b*) A. B. Canaj, S. Dey, E. R. Marti, C. Wilson, G. Rajaraman and M. Murrie, *Angew. Chem., Int. Ed.*, 2019, **58**, 14146; (*c*) Z. H. Li, Y.-Q. Zhai, W.-P. Chen, Y. S. Ding and Y.-Z. Zheng, *Chem. – Eur. J.*, 2019, **25**, 16219.

10 Recent C_n (where $n \geq 7$) examples: (*a*) D. S. Krylov, F. Liu, S. M. Avdoshenko, L. Spree, B. Weise, A. Waske, A. U. B. Wolter, B. Buchnera and A. A. Popov, *Chem. Commun.*, 2017, **53**, 7901; (*b*) F. Liu, D. S. Krylov, L. Spree, S. M. Avdoshenko, N. A. Samoylova, M. Rosenkranz, A. Kostanyan, T. Greber, A. U. B. Wolter, B. Buchner and A. A. Popov, *Nat. Commun.*, 2017, **8**, 16098.

11 A list of six-coordinate Dy(III) SMMs is located in the ESI†.

12 M. Gregson, N. F. Chilton, A.-M. Ariciu, F. Tuna, I. F. Crowe, W. Lewis, A. J. Blake, D. Collison, E. J. L. McInnes, R. E. P. Winpenny and S. T. Liddle, *Chem. Sci.*, 2016, **7**, 155.

13 B.-C. Liu, N. Ge, Y.-Q. Zhai, T. Zhang, Y.-S. Ding and Y.-Z. Zheng, *Chem. Commun.*, 2019, **55**, 9355.

14 M. Li, H. Wu, Z. Xia, L. Ungur, D. Liu, L. F. Chibotaru, H. Ke, S. Chen and S. Gao, *Inorg. Chem.*, 2020, **59**, 7158.

15 M. J. Giansiracusa, S. Al-Badran, A. K. Kostopoulos, G. F. S. Whitehead, D. Collison, F. Tuna, R. E. P. Winpenny and N. F. Chilton, *Dalton Trans.*, 2019, **48**, 10795.

16 X.-L. Ding, Y.-Q. Zhai, T. Han, W.-P. Chen, Y.-S. Ding and Y.-Z. Zheng, *Chem. – Eur. J.*, 2020, DOI: 10.1002/chem.202003931.

17 J. Long, A. N. Selikhov, E. Mamontova, K. A. Lyssenko, Y. Guari, J. Larionova and A. A. Trifonov, *Dalton Trans.*, 2020, **49**, 4039.

18 (*a*) F. Ortu, H. Zhu, M.-E. Boulon and D. P. Mills, *Inorganics*, 2015, **3**, 534; (*b*) A. Domingos, M. R. J. Elsegood, A. C. Hillier, G. Lin, S. Y. Liu, I. Lopes, N. Marques, G. H. Maunder, R. McDonald, A. Sella, J. W. Steed and J. Takats, *Inorg. Chem.*, 2002, **41**, 6761; (*c*) D.-L. Deng, Y.-H. Zhang, C.-Y. Dai, H. Zeng, C.-Q. Ye and R. Hage, *Inorg. Chim. Acta*, 2000, **310**, 51.

19 S. M. Cendrowski-Guillaume, G. Le Gland, M. Nierlich and M. Ephritikhine, *Organometallics*, 2000, **19**, 5654.

20 Y. K. Loh, M. Á. Fuentes, D. C. H. Do and S. Aldridge, *Angew. Chem., Int. Ed.*, 2019, **58**, 4847.

21 See the ESI† for full details.

22 Continuous shape measurement of first coordination sphere in **2Dy** gives 0.802 for O_h with all other six-coordinate polyhedra >10. See: (*a*) S. Alvarez, D. Avnir, M. Llunell and M. Pinsky, *New J. Chem.*, 2002, **26**, 996; (*b*) J. Cirera, M. Llunell, P. Alemany, D. Avnir and S. Alvarez, *J. Am. Chem. Soc.*, 2004, **126**, 1755.

23 www.nfchilton.com/cc-fit, accessed 1st November 2020.

24 D. Reta and N. F. Chilton, *Phys. Chem. Chem. Phys.*, 2019, **21**, 23567.

